ELSEVIER

Journal of Analytical and Applied Pyroylsis
34 (1995) 191 -217

JOURNAL of ANALYTICAL and APPLIED PYROLYSIS

Curie-point pyrolysis of sodium salts of functionalized fatty acids☆

Walter A. Hartgers*, Jaap S. Sinninghe Damsté, Jan W. de Leeuw

Netherlands Institute for Sea Research (NIOZ), Division of Marine Biogeochemistry, P.O. Box 59, 1790 AB Den Burg, The Netherlands

Received 9 March 1994; accepted 30 November 1994

Abstract

Selected sodium salts of functionalized fatty acids were subjected to Curie-point pyrolysis and their pyrolysis products subsequently analyzed by gas chromatography/mass spectrometry in order to study the thermal dissociation mechanisms of lipid moieties in bio- and geomacromolecules. Pyrolysis of the sodium salts of hydroxy and keto acids yields in each case a methylketone as the major product, which is generated via a concerted, six-membered ring rearrangement triggered by the functionality in the alkyl chain. The thermal dissociation of alkylbenzene and alkylthiophene moieties proceeds mainly via hydrogen abstraction at the α- and γ-carbon atoms, followed by β-scission. The ratios of the main product pairs, i.e. styrene/toluene and vinylthiophene/2-methylthiophene, are largely controlled by radical mobility during pyrolysis. The major fragmentation pathway of monounsaturated alkyl chains is β-cleavage adjacent to the double bond. The identification of both Z and E isomers of alkenes in the pyrolysates demonstrates that the initial stereospecifity of the double bond is not retained during pyrolysis. The formation of linear alkylbenzenes from non-phenylic precursor moieties (e.g. diunsaturated fatty acids) shows that specific alkylbenzenes in Curie-point pyrolysates are not always derived from monoaromatic precursors. The addition of organic or mineral matter suppresses these secondary processes. The extension of the model compound results to the recognition of specific types of pyrolysis products and their relevance to the reconstruction of structures of lipid moieties in natural biomacromolecules in kerogens and coals are discussed.

Keywords: Coal; Curie-point pyrolysis; Fatty acids; Kerogen; Pyrolysis; Pyrolysis mechanisms; Sodium salts

☆ This is NIOZ Division of Marine Biogeochemistry contribution No. 348.

* Corresponding author. Present address: Department of Environmental Chemistry (C.I.D.-C.S.I.C.), Jordi Girona 18, 08034 Barcelona, Catalonia, Spain.

SSDI 0165-2370(94)00881-7

1. Introduction

Spectroscopic methods such as solid state ^{13}C NMR and FT-IR provide insight into the chemical environment of carbon or hydrogen atoms (NMR), and reveal functional groups (IR) in bio- and geomacromolecules. Thermal and chemical degradation methods are often applied to elucidate the structures of monomers or building blocks in these high-molecular-weight substances [1–4]. In this respect, Curie-point pyrolysis (Py) in combination with gas chromatography (GC) and mass spectrometry (MS) has proved be a useful tool for the molecular characterization of both natural and synthetic macromolecules [5–9]. Curie-point pyrolysates of geomacromolecules (kerogen, coal, asphaltenes) are generally characterized by complex mixtures of aliphatic and aromatic hydrocarbons [7]. Pyrolysis studies of microscopically well-defined geological samples have revealed that homologous series of *n*-alkenes and *n*-alkanes are derived from highly aliphatic, selectively preserved biomacromolecules, which are widely distributed in algal cell walls [10–12], cuticles [9] and outer seed walls [13]. Ether-linked alkyl chains, present in the macromolecular substances of the outer cell walls of the microalga *Botryococcus braunii*, have been recognized and chemically characterized by the identification of specific hydrocarbons, aldehydes and ketones generated on Curie-point pyrolysis [8,14].

This study aims at obtaining a better understanding of the thermal degradation mechanisms of functionalized alkyl chains in kerogens and coals. For this purpose, model compounds representing well-defined functionalized moieties, supposed to be present in kerogen, are selected. To prevent simple evaporation of such model compounds during pyrolysis, they should either be covalently linked to a polymeric framework or be derivatized in such a way that they cannot evaporate and, consequently, are pyrolyzed. Curie-point pyrolysis experiments of silicon-bound hydrocarbons, which were used as model compounds for macromolecular-bound hydrocarbon moieties, have provided insight into thermal degradation mechanisms [15]. The major products, however, were found to be formed via a rearrangement reaction of the silicon matrix. Therefore, an alternative pathway was followed using sodium salts of functionalized fatty acids. In the present study, the effect of functional groups (aromatic rings, hydroxyl groups, double bonds) on the composition of the pyrolysate is discussed. The data provide a better understanding of the complex mechanisms of pyrolysis of well-defined, functionalized alkyl moieties. Recognition of specific degradation products in pyrolysates of kerogens and coals might help to assess the chemical structures of their precursor moieties, a prerequisite for fully decoding their biological origin.

2. Experimental

2.1. Sample description

An overview of the model compounds used in this study is given in Fig. 1. Hexadecanoic acid (**I**), 12-hydroxyoctadecanoic acid (**IV**), [*R*-(*E*)]-12-hydroxy-9-

octadecenoic acid (**VI**), *threo*-9,10-dihydroxyoctadecanoic acid (**VII**), (*Z*)-9-octadecenoic acid (**VIII**) and (*Z*,*Z*)-9,12-octadecadienoic acid (**IX**) were commercially available (Sigma). 12-Hydroxyoctadecanoic acid (**IV**, methyl ester) was oxidized with 1.5 eq. of pyridinium chlorochromate in dichloromethane (room temperature; 2 h) to 12-oxo-octadecanoic acid (**V**) in 80% yield. The absence of a multiplet at 3.6 p.p.m. (CH–OH) in the ^{1}H NMR spectrum of 12-oxo-octadecanoic acid (**V**) confirmed a complete conversion of the hydroxyl group of the starting compound into an oxo group. 16-(4′-methylphenyl)hexadecanoic acid (**II**) was synthesized as follows. 16-Oxohexadecanoic acid, prepared by oxidation (PCC; 2 h; room tem-

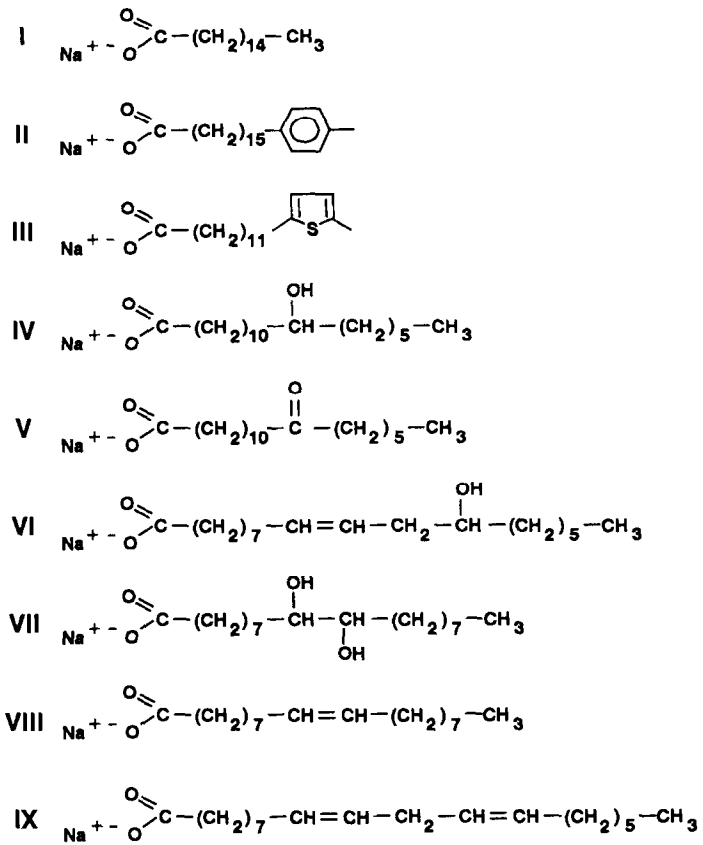

Fig. 1. Structures of sodium salts of (**I**) hexadecanoic acid, (**II**) 16-(4′-methylphenyl)hexadecanoic acid, (**III**) 12-[2′-(5′-methylthienyl)]dodecanoic acid, (**IV**) 12-hydroxyoctadecanoic acid, (**V**) 12-oxo-octadecanoic acid, (**VI**) [*R*-(*E*)]-12-hydroxy-9-octadecenoic acid, (**VII**) *threo*-9,10-dihydroxyoctadecanoic acid, (**VIII**) (*Z*)-9-octadecenoic acid and (**IX**) (*Z*,*Z*)-9,12-octadecadienoic acid.

perature) of 16-hydroxyhexadecanoic acid (Aldrich), was coupled via a Grignard reaction with 4-bromomagnesiumtoluene (5 eq.) in dry tetrahydrofuran (reflux, 2 h) and purified by column chromatography yielding the product in 60% yield. The hydroxyl group in the product was reduced using triethylsilane and BF_3·etherate [16]. The structure of 16-(4′-methylphenyl)hexadecanoic acid was confirmed by ^{1}H NMR (Ar–H, 7.07 (s, 4H); Ar–CH_2–, 3.65 (t, 2H); carboxyl–CH_2–, 2.55 (t, 2H); CH_3–Ar, 2.31 (s, 3H); –CH_2–, 1.62 (sextet, 2H); –CH_2–, 1.58 (m, 2H); –CH_2–, 1.25 (m, 22H)). Chemical shifts were determined in $CDCl_3$ and are the δ values relative to the TMS standard. 12-[2′-(5′-methylthienyl)]dodecanoic acid (**III**) was kindly provided by Dr. P. Albrecht (Université de Strasbourg, Strasbourg, France). The purity of all the model compounds used was verified by converting the free acids to their methylesters using diazomethane in diethyl ether, followed by analysis of the methylesters using GC/MS and, in some cases, ^{1}H NMR.

The free acids were converted to their sodium salts by adding 1.5 eq. of NaOH to their water-suspended solutions and stirring overnight at room temperature. The water was removed by freeze-drying the samples.

A kerogen sample of the Oligocene Kishenehn Formation (Montana, USA) was kindly donated by Dr. E.W. Tegelaar (ARCO Expl. and Prod. Techn., Plano, TX). The kerogen was isolated using HCl and HF, and subsequently extracted with methanol and dichloromethane/methanol (9:1; six times) and dried overnight under vacuum at 40°C. The clay sample (montmorillonite K 10) was commercially available (Aldrich). The clay was ultrasonically extracted three times with methanol/dichloromethane (1:1) and dried before use. In some experiments the sodium salt of 12-[2′-(5′-methylthienyl)]dodecanoic was thoroughly mixed with the kerogen or clay in a weight ratio of 1:1 using a pestle and mortar.

2.2. Pyrolysis methods

Curie point pyrolysis–gas chromatography (Py–GC) was performed using a FOM-4LX Curie-point pyrolysis unit directly connected to the injector of a Hewlett-Packard 5890 Series II gas chromatograph. The samples were pressed onto the ferromagnetic wire using a KBr press according to the method described by Venema and Veurink [17]. The on-line pyrolysis experiment was performed by inductive heating of the ferromagnetic wires to their Curie temperature at which they were held for 10 s using a high frequency generator (Fischer, model 9425). The Curie temperature was 358°C for so-called thermal extraction and 770°C for pyrolysis. Separation of the pyrolysis products was achieved by a fused silica column (25 m × 0.32 mm i.d.) coated with CP Sil-5 (film thickness 0.45 μm). Helium was used as carrier gas. The oven was programmed from 0°C (5 min) to 320°C (10 min) at a rate of 3°C/min.

Curie-point pyrolysis–gas chromatography/mass spectrometry (Py–GC/MS) was performed under the same conditions as described for Py–GC, using a similar Curie-point device and gas chromatograph to those described above coupled to the

EI ion source of a VG-70s double focusing mass spectrometer (mass range *m/z* 40–800; cycle time 2 s; ionization energy 70 eV) or a VG Autospec Ultima (mass range *m/z* 45–900; cycle time 1 s; ionization energy 70 eV).

3. Results

Fig. 1 shows an overview of the model compounds that have been studied by Py–GC and Py–GC/MS. The carboxyl group was converted to the corresponding sodium salt to prevent evaporation of the model compound under Curie-point pyrolysis conditions.

Considering the lower bond dissociation energy of C–C bonds (about 334 kJ/mol) relative to the dissociation energies of C–H bonds (about 420 kJ/mol) and C–O bonds (about 340 kJ/mol), the *initiation* step in the thermal dissociation of the model compounds studied should occur by homolytic C–C cleavages rather than by C–H or C–O cleavages. The radicals formed by these initiation steps are propagated by β-scission reactions, in which C–C bonds are broken, and by hydrogen abstraction, in which the substrate is activated and new radicals are formed.

3.1. Sodium salt of hexadecanoic acid

The Curie-point pyrolysis of the sodium salt of hexadecanoic acid (**I**) yields homologous series of *n*-alk-1-enes and *n*-alkanes up to C_{15} (Fig. 2). The low amounts of hexa- and heptadec-1-ene are due to the presence of small amounts of the sodium salt of octadecanoic acid in the sample. The generation of *n*-alk-1-enes and *n*-alkanes is in accordance with previously reported results [18,19]. No aromatic products were detected. The absence of *n*-alkanes and *n*-alk-1-enes on thermal extraction at 358°C confirmed that these products did not simply evaporate from the wire during the pyrolysis experiment. Scheme 1 outlines the proposed mechanisms of pyrolysis for the formation of these *n*-alk-1-enes and *n*-alkanes. Initiation occurs by homolysis of the weakest C–C bond adjacent to the carboxyl group. The pentadecyl radical generated is propagated either as pentadecane by intermolecular H-radical transfer reactions or is stabilized as a secondary radical by "scrambling" (random delocalization) of the primary radical along the alkyl chain. Experimental evidence [20] has demonstrated that a 1,5-hydrogen shift leading to a secondary radical is more rapid than β-scission of the primary radical at 500°C. Stabilization of the "free" secondary radicals can occur either via intermolecular H-radical transfer reactions, yielding pentadecane, or by β-scission reactions, generating a homologous series of *n*-alk-1-enes up to C_{14} and *n*-alkanes up to C_{13}. Competition between hydrogen transfer reactions to start a new chain cycle and the β-scission of any radical controls the size of products in the pyrolysate. β-Scission will be favoured over H-radical abstraction at elevated temperatures and low H-radical concentrations during thermal dissociation experiments [21].

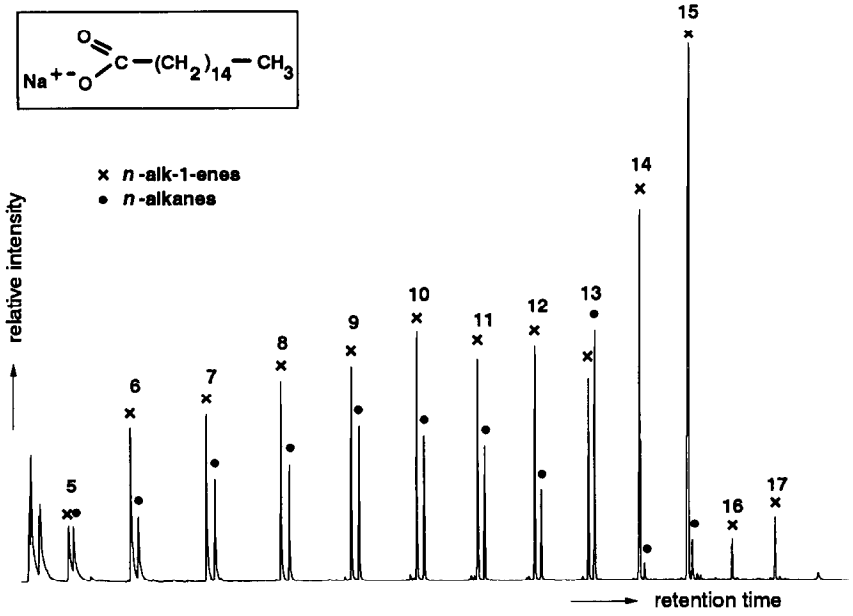

Fig. 2. Gas chromatogram of the Curie-point pyrolysate (Curie temperature = 770°C) of the sodium salt of hexadecanoic acid. Numbers indicate total number of carbon atoms.

Intermolecular H-radical transfer processes can also lead to the formation of alkyl radicals, which still contain the sodium salt functionality. Scrambling of the radical along the alkyl chain and subsequent cleavages of the allylic C–C bonds generate a homologous series of *n*-alk-1-enes up to C_{15} (Scheme 1; propagation

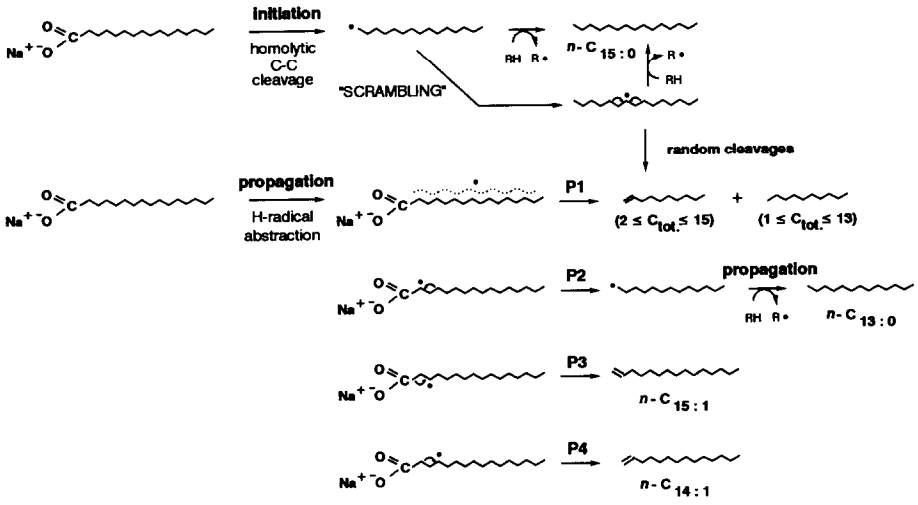

Scheme 1. Proposed mechanism of thermal degradation of the sodium salt of hexadecanoic acid.

route P1). The other products of this process, primary radicals, are thought to be stabilized by intermolecular H-radical reactions leading to the formation of *n*-alkanes up to C_{13} or via loss of a hydrogen radical to the corresponding *n*-alk-1-enes. Stabilization of secondary radicals via loss of a hydrogen radical is considered less favourable than allylic C–C cleavage, as judged from the small amounts of mid-chain alkenes in the pyrolysate. The relatively low ratio of *n*-alkanes/*n*-alk-1-enes seems to indicate a low concentration of free H-radicals, so that stabilization of the alkyl radicals as *n*-alk-1-enes is favoured.

A careful examination of the product distribution of the Curie-point pyrolysate of the sodium salt of hexadecanoic acid (**I**) reveals that the relative abundances of tridecane, tetradec-1-ene and pentadec-1-ene are enhanced. This phenomenon can be rationalized by a preference of the secondary radical for specific positions on the alkyl chain controlled by the carboxyl functionality. Secondary radicals at the α-, β- and γ-carbon atoms are favoured and induce homolytic β-scissions explaining the higher abundances of tridecane, pentadec-1-ene and tetradec-1-ene, respectively (Scheme 1; propagation routes P2–P4). The relative abundances of tridecane and tetradec-1-ene via routes P2 and P4, respectively, are in accordance with the preferred formation of $(n-2)$-alkanes and $(n-1)$-alkenes observed in pyrolysates of alkylbenzenes with alkyl chains of n carbon atoms (Ref. [22] and results described in Section 3.2).

It is noted that the low abundance of tetradecane and pentadecane is a direct result of the fragmentation pathways postulated above. The formation of pentadecane and tetradecane can only be explained by homolytic cleavage of the C_γ–C_β bond and C_β–C_γ bond relative to the carboxylic group, respectively, and subsequent intermolecular H-radical transfer processes.

3.2. Sodium salt of 16-(4′-methylphenyl)hexadecanoic acid

Fig. 3(A) shows the gas chromatogram of the Curie-point pyrolysate of the sodium salt of 16-(4′-methylphenyl)hexadecanoic acid (**II**). This compound was synthesized to study the thermal degradation behaviour of alkylbenzene moieties. On Curie-point pyrolysis, homologous series of 4-alkyltoluenes and 4-alkenyltoluenes with chain lengths of up to 15 carbon atoms are generated. The 4-alkenyltoluenes elute before their saturated equivalents, suggesting that the double bonds are located at the ω-position. Some isomerization of the terminal double bond takes place as judged from the presence of small amounts of $(\omega-1)$-alkenyltoluenes (Fig. 3(A); ◇). The formation of 4-alkyltoluenes and 4-alkenyltoluenes is thought to result from homolytic C–C cleavages of the alkyl chain and subsequent stabilization reactions by intermolecular H-radical transfers (Scheme 2; propagation route P1), similar to the thermal degradation pathways proposed for the sodium salt of hexadecanoic acid (**I**). Similarly, the higher abundances of 4-methylphenyltridecane, 4-methylphenyltetradec-1-ene and 4-methylphenylpentadec-1-ene can be explained by a preference of the location of the radical at the α-, β- and γ-carbon atoms relative to the carboxyl functionality (Scheme 2; propagation routes P2–P4). In contrast with the pyrolysate of the sodium salt of hexadecanoic acid (**I**), the alkyl chain of the major pyrolysis product of the sodium salt of 16-(4′-

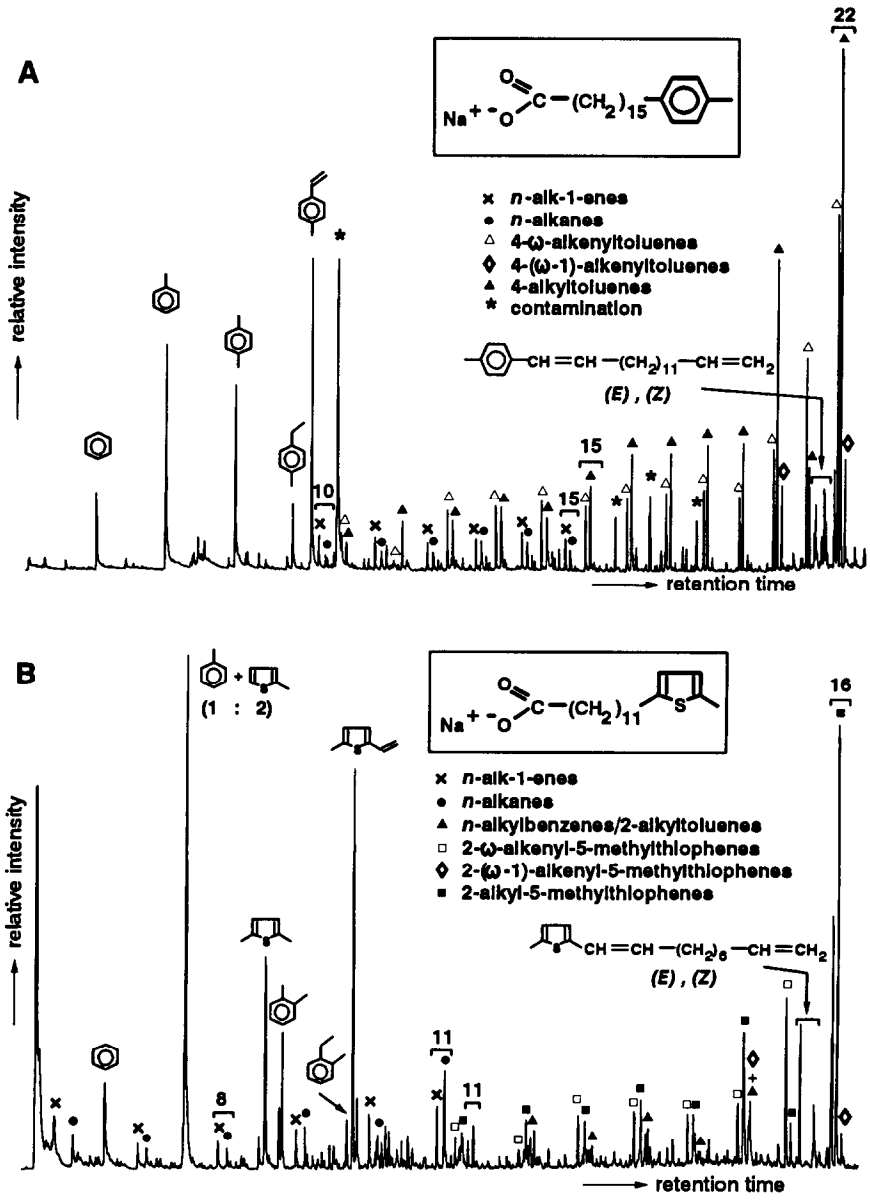

Fig. 3. Gas chromatograms of the Curie-point pyrolysates (Curie temperature = 770°C) of sodium salts of (A) 16-(4′-methylphenyl)hexadecanoic acid and (B) 12-[2′-(5′-methylthienyl)]dodecanoic acid. Numbers indicate total number of carbon atoms.

methylphenyl)hexadecanoic acid (II), 4-methylphenylpentadecane, is saturated. This phenomenon is rationalized by a relatively higher stability of the 4-methylphenylpentadecyl radical generated (Scheme 2; initiation route), causing a higher susceptibility towards a quenching reaction by H-donors (RH in Scheme 2).

The thermal dissociation behaviour of the sodium salt of 16-(4′-methylphenyl)hexadecanoic acid (**II**) is, in addition to the sodium salt functionality, governed by the presence of the aromatic moiety. The degradation pathway generally proposed for macromolecular-bound aromatic moieties is cleavage of the carbon–carbon bond between the α- and β-carbon atoms ("β-scission") of the side chain through which the aromatic nucleus is linked [23,24]. This degradation pathway (Scheme 2, propagation route P5) is favoured since β-scission can expel a stabilized benzyl radical. Less favoured fragmentation pathways are γ- and δ-scission, leading to the formation of less stabilized radicals. This fragmentation behaviour is supported by quantum mechanical calculations of the individual bond energies of alkylbenzenes. These calculations show that addition of an aromatic

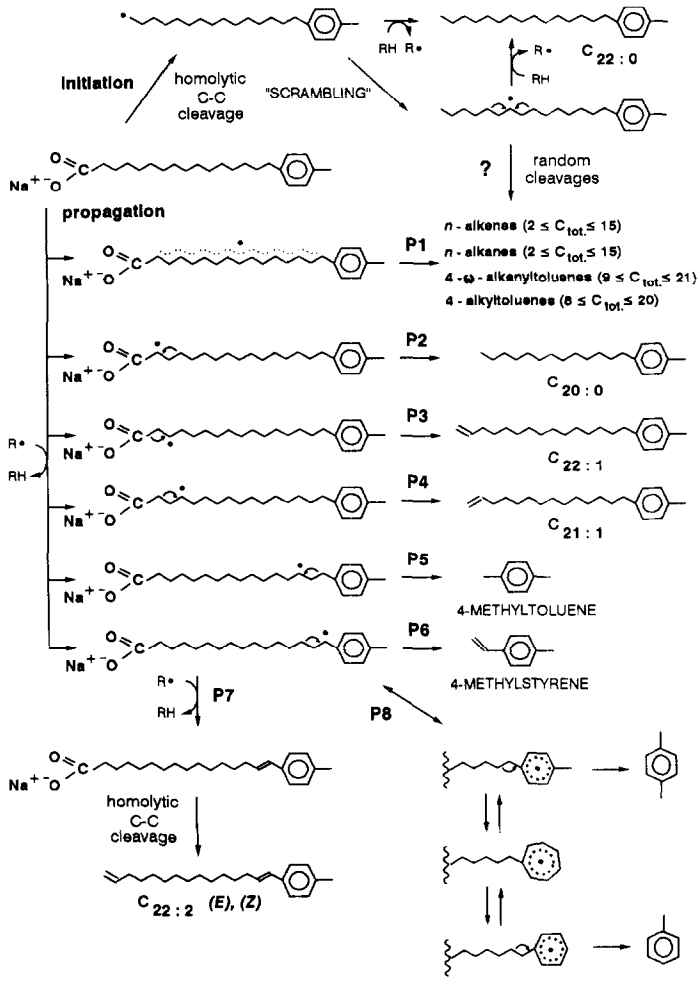

Scheme 2. Proposed mechanism of thermal degradation of the sodium salt of 16-(4′-methylphenyl)hexadecanoic acid.

nucleus strengthens the α-bond and weakens the β-bond by approximately 30 kJ/mol relative to the bond energies of aliphatic C–C bonds [25]. Macromolecular-bound alkylbenzene moieties are, thus, expected to yield a defined set of monoaromatic pyrolysis products dominated by the β-cleavage product and, to a lesser extent, γ- and δ-cleavage products. Indeed, 1,4-dimethylbenzene is found to be a major pyrolysis product of the sodium salt of **II** (Fig. 3(A)).

Contrary to these expectations is the high abundance of 4-methylstyrene in the pyrolysate. Its formation is considered to be initiated by H-radical abstraction from the carbon atom adjacent to the aromatic ring (Scheme 2; propagation route P6). Subsequent cleavage of the allylic C–C bond yields 4-methylstyrene. The preferential abstraction of the hydrogen at the α-carbon is also revealed by the presence of (*E*)- and (*Z*)-4-(pentadeca-1′,14′-dienyl)toluene in the pyrolysate, which are supposed to result from an intermolecular H-radical abstraction and subsequent homolytic C–C cleavage adjacent to the carboxyl group (Scheme 2; propagation route P7). Labelling experiments have demonstrated that the thermal dissociation of long-chain alkylbenzene moieties occurs fully via free-radical reactions comprising a sequence of radical initiation, hydrogen abstraction, β-scission, and termination steps. Neither a six-centre, intramolecular retro-ene reaction [26,27] nor a four-centre intramolecular mechanism [28] yielding toluene in a single, rate-determining concerted step can account for the formation of all the other observed products apart from toluene, and they are both ruled out by the data obtained via these labelling experiments. Thus, the overall reaction of **II** to generate 4-methyltoluene and 4-methylstryrene is clearly a function of both hydrogen abstraction and β-scission steps. Hydrogen abstraction at the α-carbon atom relative to the aromatic moiety (C–H bond energy = 356 kJ/mol) is kinetically preferred over abstraction of hydrogen atoms in the alkyl chains, which are roughly equal in reactivity (C–H bond energy = 397 kJ/mol) [29]. Consequently, a preferential hydrogen abstraction at the α-carbon and subsequent β-scission lead to the formation of relatively higher amounts of 4-methylstyrene (Scheme 2; propagation route P6). Hydrogen abstraction at the other carbon atoms of the alkyl chain should be roughly equivalent. If hydrogen abstraction was the only rate-determining step, 4-methyltoluene would be a minor product found in roughly equimolar amounts as the monoaromatic products resulting from β-scission of all non-α-hydrogen abstracted radicals. However, abstraction of the γ-hydrogen is also favoured, as β-scission leads to the formation of a resonance-stabilized benzyl radical, explaining the high abundance of 4-methyltoluene (Scheme 2; propagation route P5). This radical will undergo mainly β-scission at the α-position (C–C bond energy is about 289 kJ/mol) rather than at the δ-position (C–C bond energy is about 343 kJ/mol) [29]. This is substantiated by the low abundance of 4-butenyltoluene in the pyrolysate (Fig. 3(A)). In conclusion, product selectivity is largely controlled by the relative stabilities of the *transition states for* β-scission. This is possible only if interconversion of radicals by intra- and intermolecular hydrogen shifts occurs extensively before *β-scission* [21]. Although abstraction of the α-hydrogen leads to the formation of a more stable radical, the formation of a γ-hydrogen abstracted radical favours β-scission, because it involves the expulsion of a stabilized benzyl radical. As

mentioned above, the enhanced formation of 4-tridecyltoluene and 4-tetradec-ω-enyltoluene via routes P2 and P4, respectively, as well as the enhanced formation of 4-methyltoluene and 4-methylstyrene via routes P5 and P6, respectively, are in full agreement with literature data on the pyrolysis of long-chain alkylaromatic hydrocarbons [21,22,30]. Homologous series of *n*-alkanes and *n*-alk-1-enes up to C_{15}, which are present in the pyrolysate in relatively low amounts, are thought to be secondary reaction products resulting from the thermal degradation of alkyl chains containing the sodium salt functionality, remaining after abstraction of the aromatic moiety as described above. Obviously, these reactions show no selectivity considering the regular distribution pattern of the *n*-alkanes and *n*-alk-1-enes in the pyrolysate (Fig. 3(A)).

The presence of toluene and benzene in the pyrolysate is remarkable, as the formation of these products would require scission of the relatively strong α-bond and demethylation of the aromatic ring. Alternatively, the secondary radical can "migrate" into the aromatic nucleus. This process is favoured by the formation of a tropylium radical (Scheme 2; propagation route P8) and subsequent reallocation of the carbon–carbon bonds can possibly account for the formation of toluene. Ring closure and aromatization of the alkyl chain, however, cannot be excluded as an alternative route for the formation of toluene and might be the main route for the formation of benzene.

3.3. Sodium salt of 12-[2′-(5′-methylthienyl)]dodecanoic acid

To investigate the extent to which benzene and toluene are derived from the aromatic nucleus or from ring closure and aromatization reactions of the alkyl chain of the sodium salt of 16-(4′-methylphenyl)hexadecanoic acid (**II**), the degradation behaviour of the sodium salt of 12-[2′-(5′-methylthienyl)]dodecanoic acid (**III**) was investigated. The distribution of organic sulphur compounds generated from the Curie-point pyrolysis of **III** (Fig. 3(B)), containing a thiophene moiety instead of a phenyl moiety, is very similar to the alkylbenzene distribution in the pyrolysate of the sodium salt of 16-(4′-methylphenyl)hexadecanoic acid (**II**). The pyrolysate is characterized by homologous series of 2-alkyl-5-methylthiophenes and 2-alk-ω-enyl-5-methylthiophenes up to 16 carbon atoms. The double bonds in the alkyl chain of the latter compound class are likely to be located at the ω-position, considering their retention time behaviour. Some isomerization of the ω-double bond to the more stable ($\omega - 1$) position has also taken place. The volatile products of the pyrolysate are dominated by 2-methyl-5-vinylthiophene, 2,5-dimethylthiophene and 2-methylthiophene. The distribution of degradation products suggests that this model compound is thermally degraded in an analogous way to the sodium salt of 16-(4′-methylphenyl)hexadecanoic acid (**II**). The abundance of 4-methylstyrene and 2-methyl-5-vinylthiophene demonstrates that abstraction of an H-radical α to the aromatic nucleus is an important process. This is supported by the presence of the E and Z isomers of 4-(pentadeca-1′,14′-dienyl)toluene and 2-(deca-1′,9′-dienyl)-5-methylthiophene, respectively (Figs. 3(A) and 3(B)). Moreover, the occurrence of 2-methylthiophene demonstrates that toluene in the py-

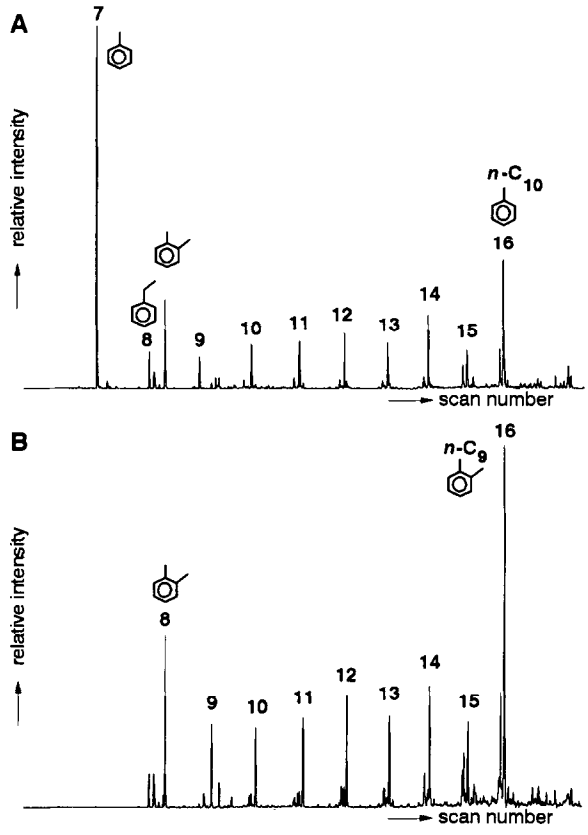

Fig. 4. Summed accurate mass chromatograms of (A) m/z 91 + 92 and (B) m/z 105 + 106 showing the distributions of n-alkylbenzenes and n-alkyltoluenes. Numbers indicate total number of carbon atoms.

rolysate of the sodium salt of 16-(4′-methylphenyl)hexadecanoic acid (**II**) is, indeed, partly derived from the aromatic moiety.

Benzene, toluene and homologous series of n-alkylbenzenes and n-alkyltoluenes with up to 16 carbon atoms are also detected as important products in the pyrolysate of the sodium salt of 12-[2′-(5′-methylthienyl)]dodecanoic acid (**III**). Their internal distributions are revealed by summed mass chromatograms of their characteristic ions (Figs. 4(A) and 4(B)). The maximum number of carbon atoms (16) and the linear carbon skeletons of the alkylbenzenes suggest that these compounds are derived from internal cyclization and aromatization reactions of the carbon skeleton of **III**. The relatively high intensities of these so-called "linear" alkylbenzenes (i.e. n-alkylbenzenes and n-alkyltoluenes), with chains containing not more than 11 carbon atoms, implies the loss of the sulphur atom, which possibly creates a reaction centre for ring closure and aromatization reactions. These reactions are schematically outlined in Scheme 3. It is believed that alkylcyclohexenes and alkylcyclohexadienes, likely intermediates, are unstable under the pyrolysis conditions used and will aromatize to yield the corresponding alkylbenzenes. It

is, therefore, concluded that benzene, toluene and "linear" alkylbenzenes in Curie-point pyrolysates can (partly) be derived from non-phenylic precursors. The absence of thiophene in the pyrolysate of the sodium salt of 12-[2'-(5'-methylthienyl)]dodecanoic acid (**III**) indicates that this mechanism might be the main source of the formation of benzene. As no aromatic hydrocarbons are encountered in the Curie-point pyrolysate of the sodium salt of hexadecanoic acid (see Fig. 2), a functional group in addition to the carboxyl moiety seems to be required for the formation of alkylbenzenes by these secondary reactions. To investigate this phenomenon further, the thermal dissociation mechanisms of other functionalized alkyl chains were examined.

3.4. Sodium salts of 12-hydroxy- and 12-oxo-octadecanoic acid

Curie-point pyrolysates of the sodium salts of 12-hydroxyoctadecanoic acid (**IV**) and 12-oxo-octadecanoic acid (**V**) exhibit highly similar product distributions (see Figs. 5(A) and 5(B)). The pyrolysate mainly consists of *n*-hexane, octan-2-one and two isomers of undecene. Tridecan-7-one and a tentatively identified branched ketone are also major pyrolysis products. The latter component was identified based on its mass spectral ($M^{\cdot+}$ 198; *m/z* 71 (base peak), 57, 58, 85, 128) and retention time behaviour. Homologous series of alkan-7-ones and alk-ω-en-7-ones[1]

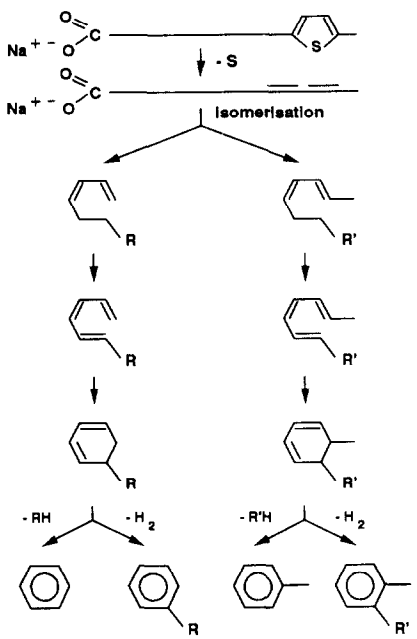

Scheme 3. Proposed mechanism explaining the formation of alkylbenzenes with linear carbon skeletons on pyrolysis of the sodium salt of 12-[2'-(5'-methylthienyl)]dodecanoic acid.

[1] For convenience the numbering of carbon atoms is started at the terminal (non-functionalized) carbon atom).

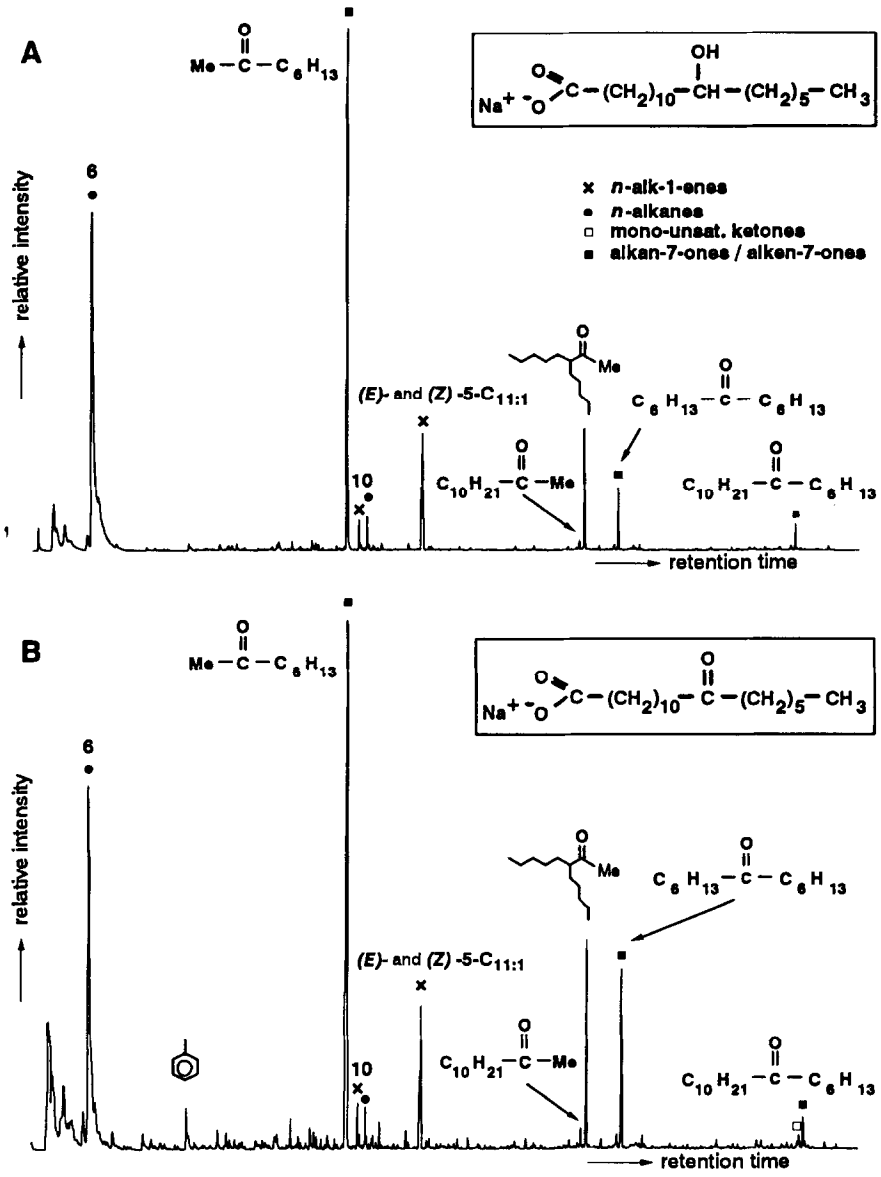

Fig. 5. Gas chromatograms of the Curie-point pyrolysates (Curie temperature = 770°C) of the sodium salts of (A) 12-hydroxyoctadecanoic acid and (B) 12-oxo-octadecanoic acid. Numbers indicate total number of carbon atoms.

are detected in the pyrolysate, although in small amounts. Toluene was detected as a minor compound in both pyrolysates.

Based on the similar pyrolysis product compositions found for both model compounds, the thermal degradation of the sodium salt of 12-hydroxyoctadecanoic

acid (**IV**) is supposed to be initiated by two H-radical abstractions allylic to the hydroxyl group and, successively, the hydroxyl-substituted carbon atom, resulting in the formation of an intermediate mid-chain ketone via the keto–enol equilibrium (Scheme 4; initiation). From now on, both model compounds **IV** and **V** are assumed to degrade via identical mechanistic pathways. The main pyrolysis product, octan-2-one, results from a six-membered ring rearrangement (Scheme 4; propagation route P1). Alternatively, homolytic cleavage of the alkyl chain adjacent to the carboxyl group generates a primary radical which can stabilize via intermolecular H-radical transfer and random cleavage of the C–C bond, resulting in the formation of homologous series of alkan-7-ones and alk-ω-en-7-ones up to C_{17}, and a series of *n*-alkanes and *n*-alk-1-enes up to C_{10}. This process (not shown in Scheme 4), however, seems to be less important as revealed by the very small amounts of these compounds in the pyrolysate. The other product resulting from the six-membered ring rearrangement (Scheme 4; propagation route P2), pent-1-ene, is not encountered as a major product in the pyrolysate. It is thought that pent-1-ene recombines almost quantitatively with the starting compound, preferentially at the α-carbon atoms at both sides of the carboxyl group (Scheme 4; recombination routes R1 and R2). The driving force for this recombination is

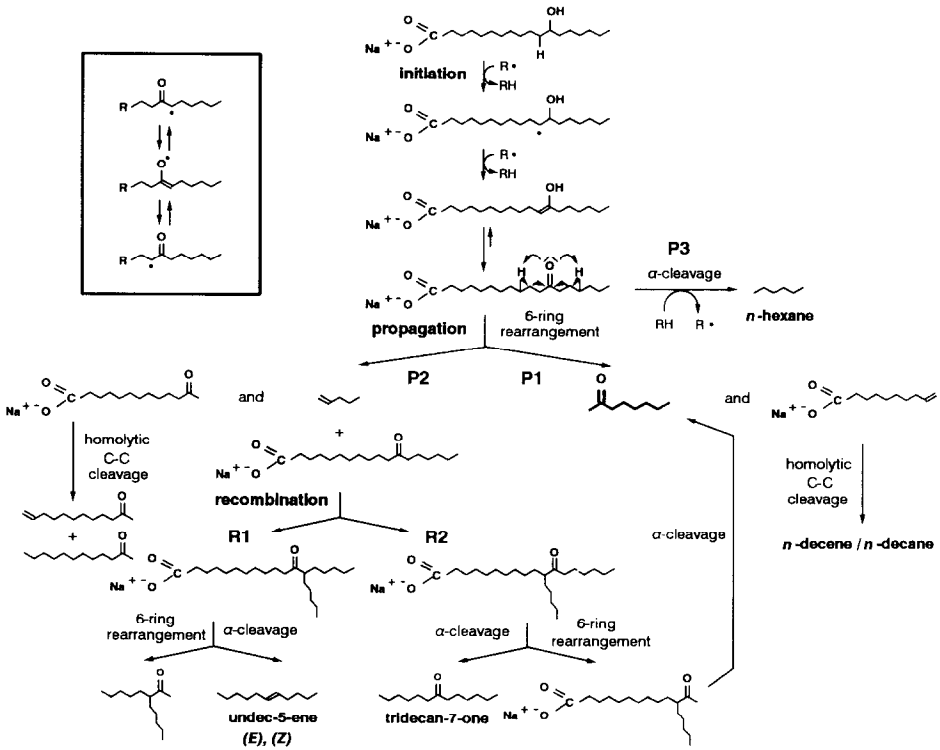

Scheme 4. Proposed mechanism of thermal degradation of the sodium salts of 12-hydroxy- and 12-oxo-octadecanoic acid. Inset shows stabilization of radicals obtained after abstraction of the α-hydrogen radical adjacent to the keto group.

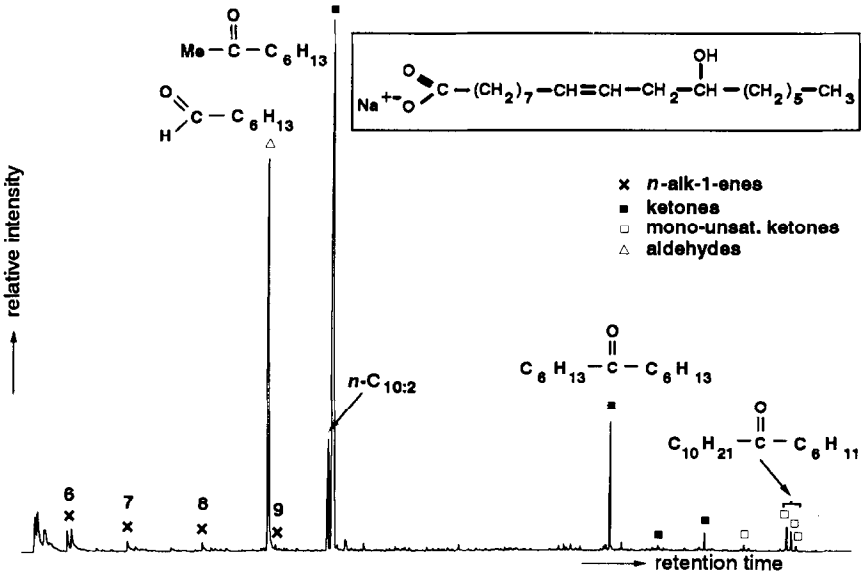

Fig. 6. Gas chromatogram of the Curie-point pyrolysate (Curie temperature = 770°C) of the sodium salt of [*R*-(*E*)]-12-hydroxy-9-octadecenoic acid. Numbers indicate total number of carbon atoms.

possibly the relative stable radical at the carbon atoms adjacent to carboxyl group (Scheme 4; inset). Consequently, tridecan-7-one, the branched C_{13} ketone and (*E*)- and (*Z*)-undec-5-ene in the pyrolysate are assumed to result from these recombination products either by a six-membered ring rearrangement or α-cleavage adjacent to the keto group. The high abundance of *n*-hexane is rationalized by α-cleavage adjacent to the keto group and subsequent stabilization by intermolecular H-radical transfer reactions (Scheme 4; propagation route P3).

3.5. Sodium salt of [R-(E)]-12-hydroxy-9-octadecenoic acid

Curie-point pyrolysis of the sodium salt of [*R*-(*E*)]-12-hydroxy-9-octadecenoic acid (**VI**; Fig. 6) yields similar products to those present in the pyrolysate of the sodium salts of 12-hydroxy- and 12-oxo-octadecanoic acid (**IV** and **V**; Fig. 5), indicating that the major fragmentation pathways are mainly controlled by the hydroxyl group in the alkyl chain. Heptanal and decadiene are also important pyrolysis products. Scheme 5 outlines the major fragmentation mechanisms of the sodium salt of [*R*-(*E*)]-12-hydroxy-9-octadecenoic acid (**VI**). As postulated above, the thermal dissociation is initialized by the abstraction of two H-radicals, yielding the sodium salt of an unsaturated keto acid (Scheme 5; initiation). Octan-2-one, the major pyrolysis product, is believed to result from a six-membered ring rearrangement (Scheme 5; propagation route P1). The formation of tridecan-7-one is proposed to follow a retro Diels–Alder reaction (Scheme 5; propagation route P2). Both rearrangements require isomerization of the double bond present, which occurs readily above temperatures of 300°C. Homolytic C–C cleavage adjacent to

the carboxyl group followed by intermolecular H-radical transfers and random cleavages of the alkyl chain is judged to be of less importance, considering the relatively low amounts of homologous series of alkenes and mid-chain ketones (Fig. 6). The formation of heptanal can be rationalized by α-cleavage adjacent to the keto group (Scheme 5; propagation route P3), which is favoured by the position of the double bond in the alkyl chain, weakening the allylic C–C bond relative to this double bond. The other product of this reaction, a primary radical, can generate decadiene by a homolytic cleavage of the C–C bond adjacent to carboxylic group followed by intermolecular H-radical transfer reactions.

3.6. *Sodium salt of* threo-*9,10-dihydroxyoctadecanoic acid*

Fig. 7 shows the gas chromatogram of the pyrolysate of the sodium salt of *threo*-9,10-dihydroxyoctadecanoic acid (**VII**). The main product generated is nonanal. Two saturated C_{10}- and C_{11}-methylketones are also abundant pyrolysis products. Homologous series of mid-chain ketones, *n*-alkanes and *n*-alk-1-enes are only present as minor compounds.

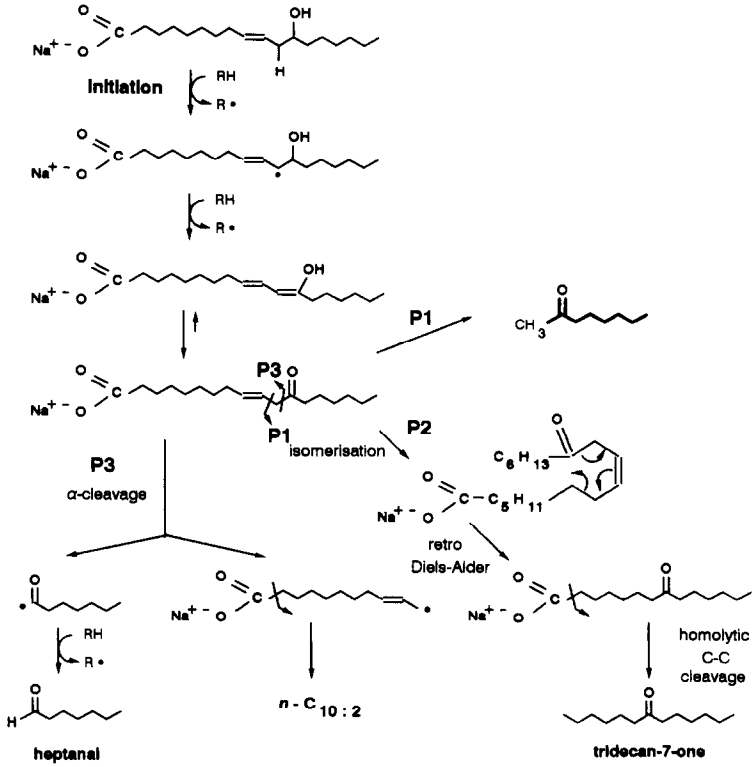

Scheme 5. Proposed mechanism of thermal degradation of the sodium salt of [*R*-(*E*)]-12-hydroxy-9-octadecenoic acid.

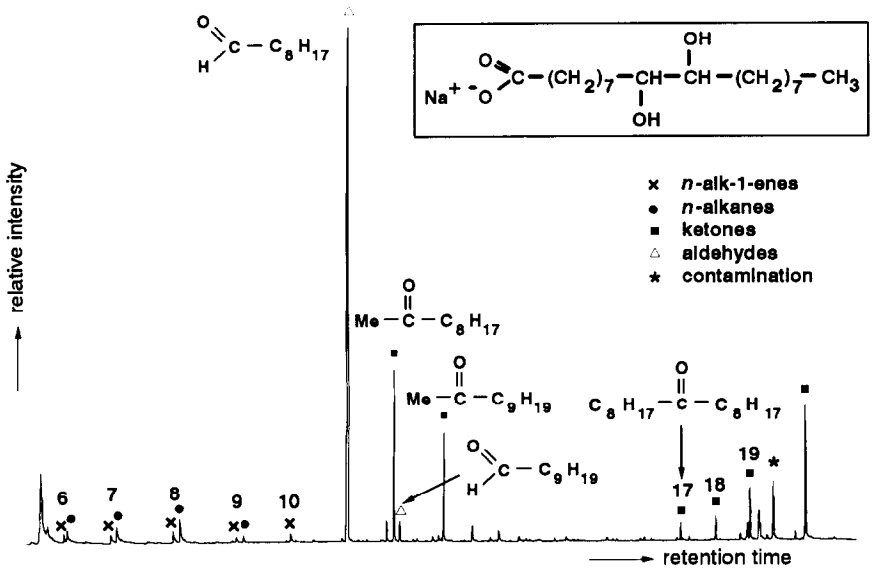

Fig. 7. Gas chromatogram of the Curie-point pyrolysate (Curie temperature = 770°C) of the sodium salt of *threo*-9,10-dihydroxyoctadecanoic acid. Numbers indicate total number of carbon atoms.

As a consequence of the presence of two adjacent hydroxyl groups in the alkyl chain, the homolytic C–C cleavage adjacent to the carboxylic group becomes unimportant. Nonanal results from a homolytic cleavage of the relatively weak bond between C_9 and C_{10} (Scheme 6; initiation). The radical generated by this cleavage can stabilize as an aldehyde. Cleavage of the bond between C_9 and C_{10} already occurs at low temperatures, as demonstrated by the generation of nonanal using ferromagnetic wires with a Curie-temperature of 358°C. The formation of decan-2-one and undecan-2-one is explained by a dehydration of the hydroxyl group at either C_9 or C_{10}, followed by a six-membered ring rearrangement (Scheme 6; propagation routes P1a and P2a) as already observed for the sodium salt of 12-oxo-octadecanoic acid (**V**). The relatively low concentration of a homologous series of mid-chain ketones and *n*-alkanes/*n*-alk-1-enes demonstrates that homolytic cleavages adjacent to the carboxyl group followed by a scrambling process of the radical yielded can be considered as less important degradation pathways (Scheme 6; propagation routes P1b and P2b). Mid-chain ketones with more than 17 carbon atoms, eluting at the end of the gas chromatogram, are supposed to be generated via similar recombination processes to those observed for the sodium salt of 12-oxo-octadecanoic acid (**V**; Scheme 4).

3.7. Sodium salts of (Z)-9-octadecenoic acid and (Z,Z)-9,12-octadecadienoic acid

The Curie-point pyrolysate of the sodium salt of (*Z*)-9-octadecenoic acid (**VIII**; Fig. 8(A)) is mainly characterized by linear alkenes up to C_{11} and linear alkadienes ranging from C_{11} to C_{17}. As well as *n*-alk-1-enes, other linear alkenes and

alkadienes with double bonds in different positions also occur in the pyrolysate. For example, in addition to undec-1-ene the E and Z isomers of undec-2-ene are also present as abundant components. The positions of the double bonds in the alkyl chains were established by comparison of their mass spectra and retention time data with those published for this class of compounds [31,32]. The E and Z isomers of four relatively abundant alkadienes were identified: 1,3-undecadiene, 1,3-dodecadiene, 1,7-hexadecadiene and 1,8-heptadecadiene (Fig. 8(A)). In all cases, the E

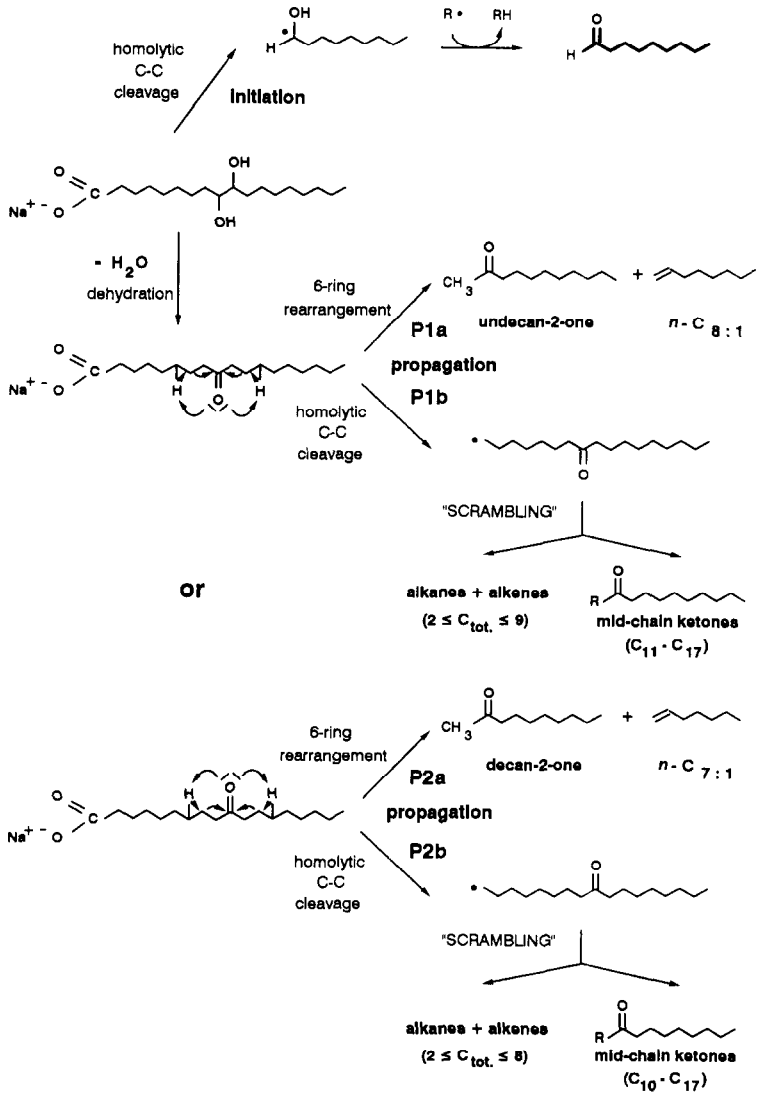

Scheme 6. Proposed mechanism of thermal degradation of the sodium salt of *threo*-9,10-dihydroxyoctadecanoic acid.

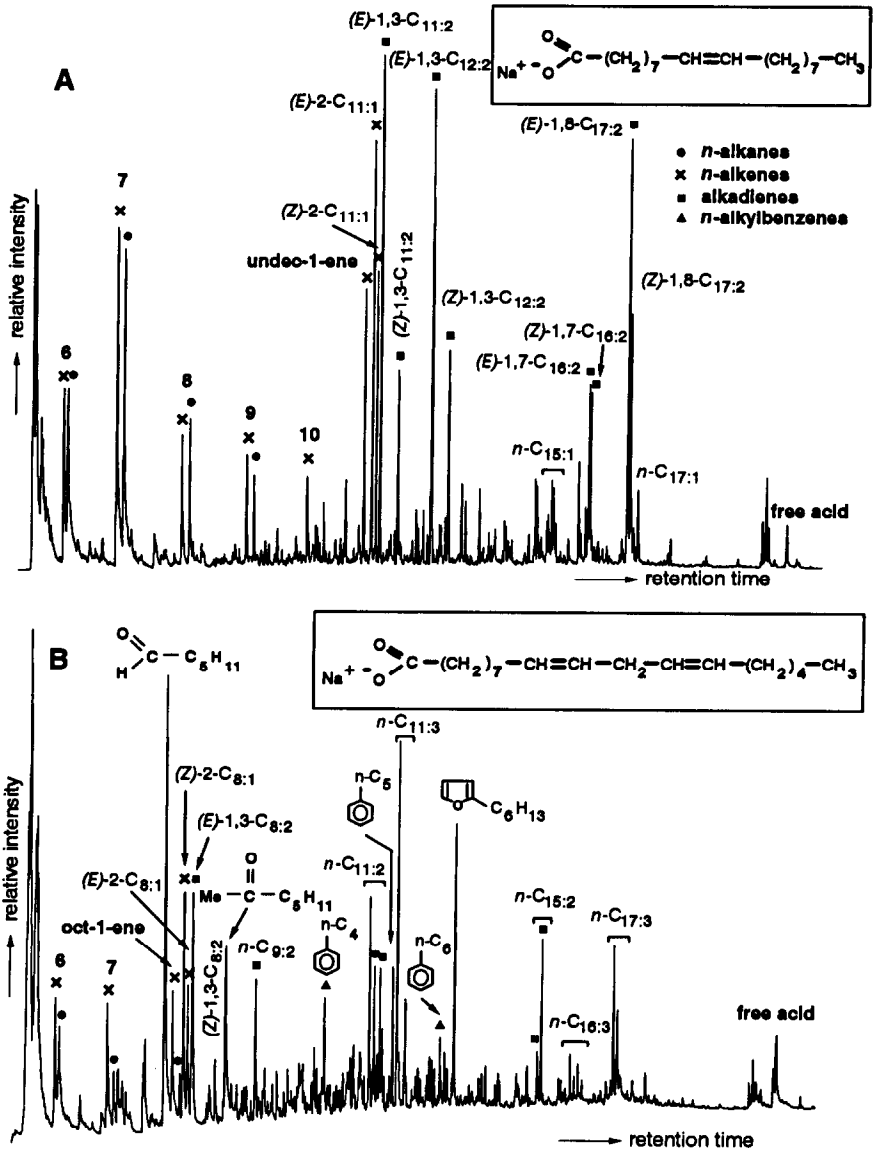

Fig. 8. Gas chromatograms of the Curie-point pyrolysates (Curie temperature = 770°C) of the sodium salts of (A) (*Z*)-9-octadecenoic acid and (B) (*Z,Z*)-9,12-octadecadienoic acid. Numbers indicate total number of carbon atoms.

isomers elute earlier than the Z isomers. The differences in retention times become smaller with increasing distance between the double bond positions in the alkyl chain. Aromatic products were detected in trace amounts only.

Scheme 7 outlines the major fragmentation mechanisms of the sodium salt of (*Z*)-9-octadecenoic acid, which are analogous to the fragmentation mechanisms

proposed for the sodium salt of hexadecanoic acid (**I**; Scheme 1). The presence of the double bond in the alkyl chain, however, favours homolytic C–C cleavages at the allylic positions (Scheme 7; initiation routes I1 and I2) rather than homolytic C–C cleavages adjacent to the carboxyl group (Scheme 7; initiation route I3) due to the lower bond dissociation energies of allylic C–C bonds. This is substantiated by the relatively high amounts of undec-1-ene, and E and Z isomers of undec-2-ene and heptane, and the low abundance of heptadec-8-ene in the pyrolysate (Fig. 8). The presence of both the E and Z isomers of undec-2-ene and undec-1-ene demonstrates that isomerization of double bonds occurs readily. A preference of the secondary radicals, generated by intermolecular H-radical transfer reactions, for specific carbon positions in the alkyl chain of (*Z*)-9-octadecanoic acid is revealed by an enhancement of specific products in the pyrolysate. The formation of E and Z isomers of 8-pentadecene, 1,8-heptadecadiene and 1,7-hexadecadiene, important pyrolysis products, is explained by the homolytic β-scission of secondary radicals at the α-, β- and γ-carbon atoms, respectively (Scheme 7; propagation routes P2, P3

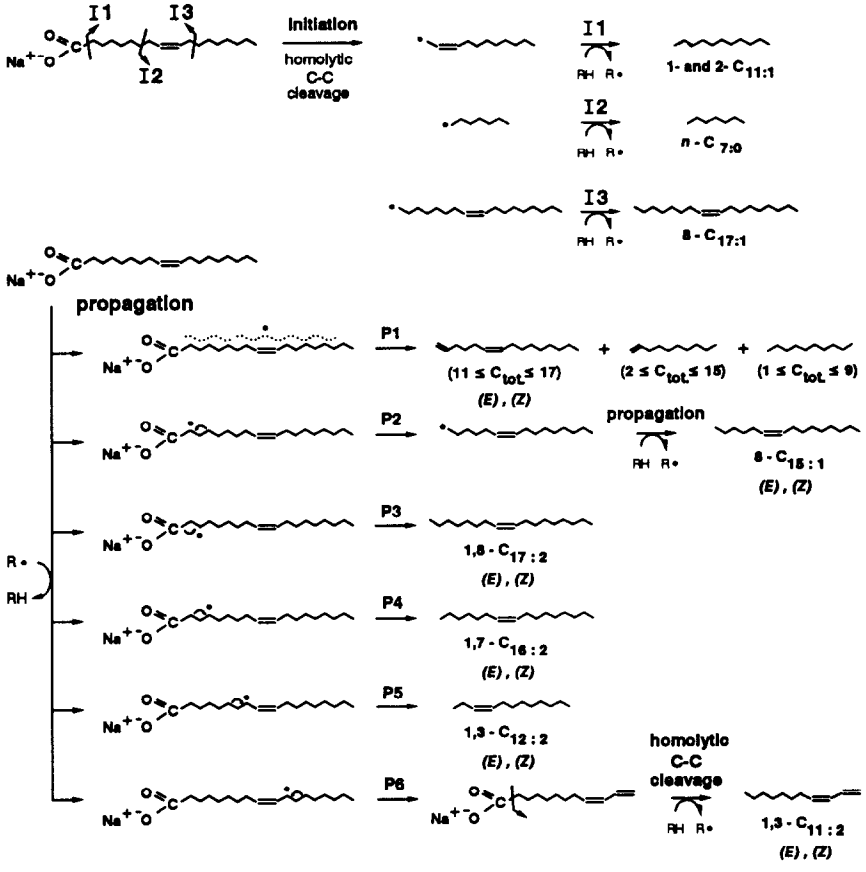

Scheme 7. Proposed mechanism of thermal degradation of the sodium salt of (*Z*)-9-octadecenoic acid.

and P4). These reaction pathways are analogous to those proposed for the sodium salt of hexadecanoic acid (**I**; see Scheme 1). The presence of the mid-chain double bond favours the formation of secondary radicals at the allylic positions which induce homolytic β-scissions, explaining the formation of the stereoisomers of 1,3-dodecadiene and 1,3-undecadiene (Scheme 7; propagation routes P5 and P6).

Fig. 8(B) shows the Curie-point pyrolysate of the sodium salt of (*Z*,*Z*)-9,12-octadecadienoic acid (**IX**). The pyrolysate is characterized by the presence of alkadienes, alkatrienes and a homologous series of *n*-alkylbenzenes. The identification of alkadienes and alkatrienes is based on mass spectral data, relative retention times and comparison of the pyrolysis products with those of (*Z*)-9-octadecenoic acid (**VIII**). A series of C_7–C_{17} *n*-alkylbenzenes is present in the pyrolysate. Their absence in experiments performed at 358°C demonstrates that these compounds are not present as such in the sample.

The C_8 cluster of alkenes and alkadienes, composed of oct-1-ene, (*E*)- and (*Z*)-2-octene, and (*E*)- and (*Z*)-1,3-octadiene, as well as the C_{11} cluster consisting of undecadienes and undecatrienes, are explained by β-cleavage of the C–C bonds adjacent to the double bonds. This is analogous to the formation of C_{11} alkenes from the sodium salt of (*Z*)-9-octadecenoic acid (**VIII**). Similarly, the enhanced amounts of pentadecadienes, hexadecatrienes and heptadecadienes in the pyrolysate indicate a preference of the secondary radical for the α-, β- and γ-carbon positions relative to the carboxyl group. The additional bond in the alkyl chain seems to favour cyclization and subsequent aromatization of the alkyl chain, similar reactions to those proposed for the formation of alkylbenzenes form the sodium salt of 12-[2′-(5′-methylthienyl)]dodecanoic acid (**III**). Obviously, the presence of two conjugated double bonds in the alkyl chain triggers the cyclization at defined positions (Scheme 3), leading to the formation of a homologous series of *n*-alkylbenzenes dominated by butyl-, pentyl- and hexylbenzene (Fig. 8(B)). Oxygen-containing compounds are significant among the pyrolysates and were identified as hexanal, heptan-2-one and 2-hexylfuran. Their occurrences are thought to be indicative of the presence of oxygen functionalities in the alkyl chain, probably introduced by oxidation of the double bonds during storage. Such reactions result in the formation of epoxy groups, keto groups and intermolecular oxygen-linkages, which upon pyrolysis yield components to some extent similar to those encountered in the pyrolysates of the sodium salts of the keto and hydroxy fatty acids discussed above.

4. Discussion

The Curie-point pyrolysis of sodium salts of functionalized fatty acids is shown to be a simple and effective method for studying the influence of functional groups in alkyl chains on the mechanism of pyrolysis and on the composition of the pyrolysate. Analysis of the degradation products of the model compounds revealed that the position and nature of functional groups in the alkyl chain dictate the series of pyrolysis products formed. Recognition of these specific degradation products and their mode of formation can provide clues to the chemical structures

of their precursor moieties in macromolecular substances, such as kerogens, coals and asphaltenes. This approach could be worthwhile, since hypothetical structures of these macromolecular substances contain similar functionalized hydrocarbon moieties joined together in an oligomeric fashion by aliphatic, naphthenic, or heteroatomic linkages [33,34].

Homolytic cleavage adjacent to the carboxylic group is relatively important if other bonds in the alkyl chain have comparable strengths. This is reflected by the abundance of homologous series of alkylbenzenes and alkylthiophenes in the pyrolysates of the sodium salts of 16-(4′-methylphenyl)hexadecanoic acid (**II**) and 12-[2′-(5′-methylthienyl)]dodecanoic acid (**III**), respectively. Similarly, the unusual distribution pattern of a series of long-chain alkylbenzenes, maximizing at C_{18}, in a coal pyrolysate, has been attributed to the presence of long-chain alkylbenzene moieties bound via a heteroatom to the coal matrix [35]. The importance of this process, however, becomes less significant if other functional groups (ester groups, keto groups, hydroxyl groups) are present in the alkyl chain. For example, the Curie-point pyrolysis of the sodium salt of 9,10-dihydroxyoctadecanoic acid (**VII**) yields nonanal as the major product, resulting from a homolytic cleavage of the relatively weak C–C bond between the carbon atoms bearing the hydroxyl groups. In cases where bonds are broken in the alkyl chain resulting in the formation of conjugated double bonds, pyrolysis products are generated which can partially result in the formation of aromatic hydrocarbons through cyclization and aromatization reactions. An interpretation of the origin and geochemical significance of specific alkylbenzenes, particularly benzene and toluene, in the Curie-point pyrolysates of kerogens and coals should, therefore, be performed with caution.

4.1. Applications to pyrolysates of macromolecular sedimentary organic matter

The thermal degradation mechanisms proposed for several model compounds in this study confirmed the results obtained by the Curie-point pyrolysis of ether lipids isolated from the green microalga *Botrycoccus braunii* [8]. Spectroscopic techniques (IR, ^{1}H NMR and ^{13}C NMR) and chemolysis experiments, such as ozonolysis, elucidated the structures of two types of ether lipids isolated from two different strains of this microalga [36]. Type I ether lipids are composed of hydroxylated alkyl moieties with unsaturations at specific positions in the alkyl chain. The structural features of these lipids show a marked analogy to the chemical structure of [*R*-(*E*)]-12-hydroxy-9-octadecenoic acid (**VI**). Their structural relationship is revealed by similar types of pyrolysis products, i.e. aldehydes and ketones, which are generated via analogous degradation pathways [8]. For example, octadecanal is proposed to result from α-cleavage adjacent to the hydroxyl group, which is favoured by weakening of this C–C bond due to an allylic double bond (see Scheme 5; route B). Type II ether lipids are comprised of long-chain alkenylalkyldimethoxyphenols linked by two adjacent ether bridges [36]. The abundance of alkanals was explained to result from homolytic C–C cleavages between the two adjacent oxygen functionalities, similar to the degradation mechanism proposed for

the sodium salt of *threo*-9,10-dihydroxyoctadecanoic acid (**VII**; Scheme 6). Recognition of the above-mentioned specific types of pyrolysis products and their mode of formation on pyrolysis revealed the chemical composition of Coorongites, shore-deposited accumulations of *B. braunii* algae at Lake Balkash (Russia). Coorongites were found to consist mainly of highly resistant aliphatic biomacromolecules (algenaens) and insoluble oxygen cross-linked substances resulting from the oxidative polymerization of ether lipids originally present as free lipids in *B. braunii* [32].

4.2. Pyrolytic behaviour of alkylaromatic moieties

Based on thermodynamic calculations [25,29], it would be expected that the favoured degradation pathway of monoaromatic compounds (i.e. long-chain alkylbenzenes, alkylthiophenes) is homolytic cleavage between the α- and β-carbon atoms (the so-called "β-scission"), as this reaction results in the formation of the most stabilized radical. The thermal degradation studies of 16-(4′-methylphenyl)hexadecanoic acid (**II**) and 12-[2′-(5′-methylthienyl)]dodecanoic acid (**III**) show, however, that there is clear competition between abstraction of the γ-hydrogen, leading to the formation of the β-cleavage product, and abstraction of the α-hydrogen, yielding vinyl-type products. This thermal degradation behaviour of monoaromatic model compounds is also observed for *n*-dodecylbenzene [30] and *n*-pentadecylbenzene [22], yielding both toluene and styrene as major products. Although vinylic compounds (i.e. styrene, vinylthiophene) have been identified in the pyrolysates of kerogens and coals [37], their concentrations are relatively low compared to products thought to result from β-cleavage (i.e. toluene, 2-methylthiophene). This discrepancy between the pyrolytic behaviour of low-molecular-weight model compounds and high-molecular-weight sedimentary organic matter might be due to diffusional limitations, which are more significant on the pyrolysis of complex, high-molecular-weight substances. It is reasonable to assume that the reactions of alkylaromatic radicals in kerogen, coal and asphaltenes will be affected by diffusion, as the diminished mobility of these radicals will locate them near their point of origin. Under such conditions, the initial rates of decomposition of alkylaromatic moieties in high-molecular-weight substances will be slower than those encountered in model compounds, thus favouring the formation of the most thermodynamically stable end products (i.e. the β-cleavage product). Consequently, the kinetically preferred hydrogen abstraction at the α-carbon atom adjacent to the aromatic nucleus will be less favoured on pyrolysis of kerogens, coals and asphaltenes. In conclusion, the pyrolysis product composition may be predominantly determined by the relative stabilities of the transition states for β-scission.

4.3. Effects of organic and mineral matter on the degradation behaviour of aromatic moieties

In addition to diffusional limitations causing differences between the pyrolytic behaviour of model compounds and high-molecular-weight sedimentary organic

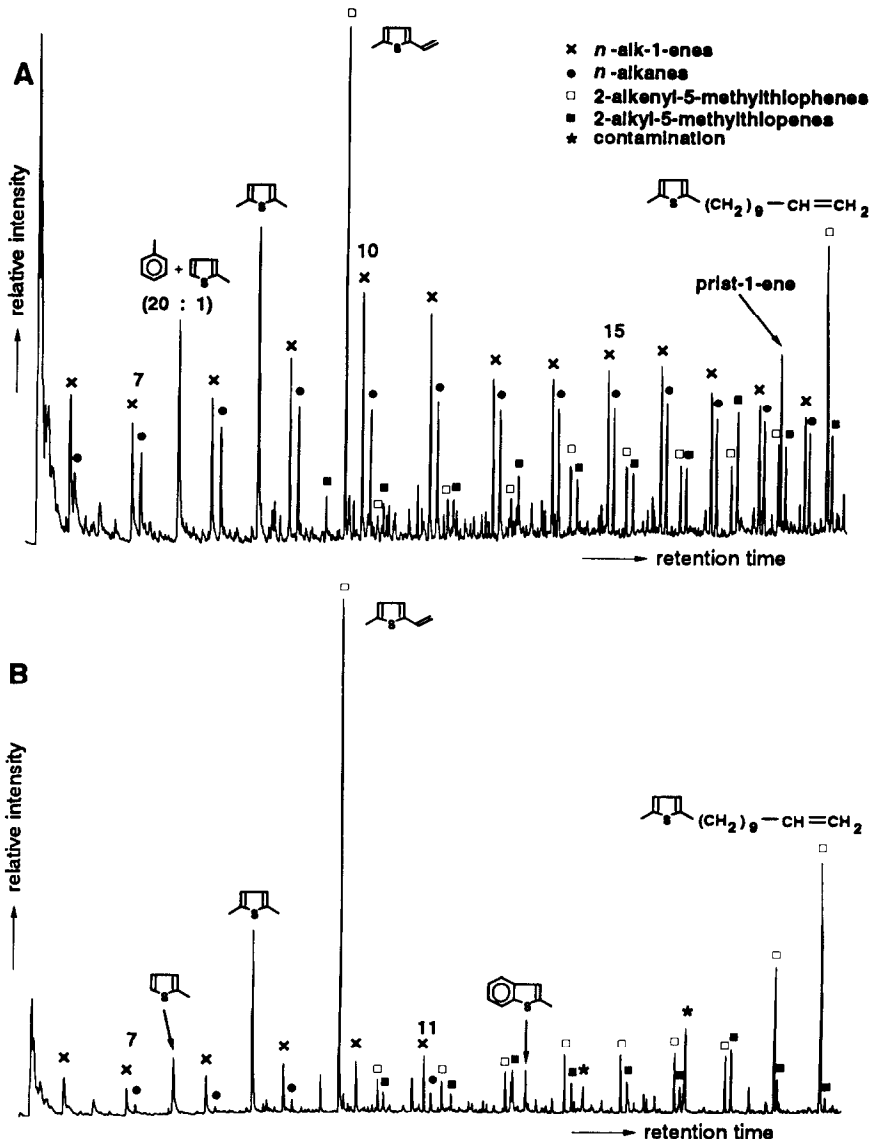

Fig. 9. Gas chromatograms of the Curie-point pyrolysates (Curie temperature = 770°C) of the sodium salt of 12-[2′-(5′-methylthienyl)]dodecanoic acid thoroughly mixed with (A) a hydrogen-rich, sulphur-poor kerogen and (B) montmorillonite clay. Numbers indicate total number of carbon atoms.

matter, clay minerals have also been reported to affect the product distribution of pyrolysates of kerogens and coals [38,39]. To study the effect of both organic and inorganic substances on the degradation behaviour of alkyl-bound aromatic moieties, the sodium salt of 12-[2′-(5′-methylthienyl)]dodecanoic acid (**III**) was thoroughly mixed with a hydrogen-rich, sulphur-poor kerogen and with a

montmorillonite clay. The major pyrolysis products of the kerogen are prist-1-ene and homologous series of *n*-alk-1-enes and *n*-alkanes, but sulphur compounds are absent. Curie-point pyrolysis of the model compound mixed with this kerogen sample (Fig. 9(A)) and the clay sample (Fig. 9(B)) revealed in each case that 2-methyl-5-vinylthiophene was still the most dominant pyrolysis product. Further, the series of 2-alkenyl-5-methylthiophenes became more important relative to their saturated counterparts. This trend was also observed for the homologous series of *n*-alkanes and *n*-alk-1-enes generated from the isolated kerogen. The relative amounts of 2-methylthiophene, thiophene and alkylbenzenes, however, decreased significantly. This observation seems to indicate that secondary processes, such as ring closure and aromatization reactions of acyclic precursors, are suppressed by the presence of organic and mineral matter. Although the changes in the composition of the pyrolysate reflect more accurately the degradation behaviour of (mono)aromatic moieties in sedimentary matter, a discrepancy still remains. Obviously, factors controlling their degradation behaviour, such as mode of binding or the effect of water generated on pyrolysis, are not fully perceived yet.

Acknowledgements

Dr. P. Albrecht (Université de Strasbourg) and Dr. E.W. Tegelaar (ARCO) are acknowledged for providing samples. Dr. A. Sinnema is acknowledged for NMR measurements. Mr. W. Pool and Mrs. M. Dekker are thanked for technical assistance. Dr. P.F. Britt is thanked for helpful discussions during preparation of the manuscript. Substantial contributions from the anonymous reviewers significantly improved this paper.

References

[1] J. Rullkötter and W. Michaelis, Org. Geochem., 16 (1990) 829.
[2] J.K. Whelan and C.L. Thompson-Rizer, in M.H. Engel and S.A. Macko (Eds.), Organic Geochemistry, Principles and Applications, Plenum, New York, 1993, p. 289.
[3] G. Standen and G. Eglinton, Chem. Geol., 97 (1992) 307.
[4] M.C. Terrón, M.L. Fidalgo, A.E. González, G. Almendros and G. Galletti, J. Anal. Appl. Pyrolysis, 27 (1993) 57.
[5] Y. Cohen and Z. Aizenshtat, J. Anal. Appl. Pyrolysis, 22 (1992) 153.
[6] T.P. Wampler and E.J. Levy, Analysts, 111 (1986) 1065.
[7] S.R. Larter and B. Horsfield, in M.H. Engel and S.A. Macko (Eds.), Organic Geochamistry, Principles and Applications, Plenum, New York, 1993, p. 271.
[8] F. Gelin, J.-P.L.A. Gatellier, J.S. Sinninghe Damsté, P. Metzger, S. Derenne, C. Largeau and J.W. de Leeuw, J. Anal. Appl. Pyrolysis, 27 (1993) 155.
[9] E.W. Tegelaar, J.W. de Leeuw and P.J. Holloway, J. Anal. Appl. Pyrolysis, 15 (1989) 289.
[10] S. Derenne, C. Largeau, C. Berkaloff, B. Rousseau, C. Wilhelm and P.G. Hatcher, Phytochemistry, 31 (1992) 1923.
[11] S. Derenne, P. Metzger, C. Largeau, P.F. van Bergen, J-P.L.A. Gatellier, J.S. Sinninghe Damsté, J.W. de Leeuw and C. Berkaloff, Org. Geochem., 19 (1992) 299.
[12] K. Goth, J.W. de Leeuw, W. Püttmann and E.W. Tegelaar, Nature, 336 (1988) 759.

[13] P.F. van Bergen, M.E. Collinson, J.S. Sinnignhe Damsté and J.W. de Leeuw, Geochim. Cosmochim. Acta, 58 (1994) 231.
[14] F. Gelin, J.W. de Leeuw, J.S. Sinninghe Damsté, S. Derenne, C. Largeau and P. Metzger, Org. Geochem., 21 (1994) 423.
[15] W.A. Hartgers, J.S. Sinninghe Damsté and J.W. de Leeuw, J. Anal. Appl. Pyrolysis, 20 (1991) 141.
[16] D.N. Kursanov, Z.N. Parnes, G.I. Bolestova and L.I. Belen'kii, Tetrahedron, 31 (1975) 311.
[17] A. Venema and J. Veurink, J. Anal. Appl. Pyrolysis, 7 (1985) 207.
[18] A.M. Shedrinsky, R.E. Stone and N.S. Baer, J. Anal. Appl. Pyrolysis, 20 (1991) 229.
[19] A. Shimoyama and W.D. Johns, Geochim. Cosmochim. Acta, 26 (1972) 87.
[20] M.L. Poutsma and S.R. Schaffer, J. Phys. Chem., 77 (1973) 158.
[21] M.L. Poutsma, Energy Fuels, 4 (1990) 113.
[22] P.E. Savage and M.T. Klein, Ind. Eng. Chem. Res., 26 (1987) 488.
[23] J.S. Sinninghe Damsté, T.I. Eglinton, J.W. de Leeuw and P.A. Schenck, Geochim. Cosmochim. Acta, 53 (1989) 873.
[24] A.G. Douglas, J.S. Sinninghe Damsté, M.G. Fowler, T.I. Eglinton and J.W. de Leeuw, Geochim. Cosmochim. Acta, 55 (1991) 275.
[25] M.J. Claxton, R.L. Patience and P.J.D. Park, in K. Øygard (Ed.), Organic Geochemistry, Poster sessions from the 16th International Meeting on Organic Geochemistry, Stavanger, 20–24 September, 1993, Falch Hurtigtrykk, Oslo, 1993, p. 198.
[26] C. Rebick, in A.G. Oblad, H.G. Davis and R.T. Eddinger (Eds.), Advances in Chemistry No. 170, Am. Chem. Soc., Washington, DC, 1979, p. 1.
[27] M.T. Klein and P.S. Virk, Ind. Eng. Chem., Fundam., 22 (1985) 35.
[28] B. Blouri, F. Handam, and D. Herault, Ind. Eng. Chem., Process Des. Dev., 24 (1985) 30.
[29] S.W. Benson, Thermochemical Kinetics, Wiley, New York, 1976.
[30] K. Derge, Chem. Ztg., Chem. Appar., 91 (1967) 729.
[31] J.-E. Dubois, J.R. Chrétien, L. Soják and J.A. Rijks, J. Chromatogr., 194 (1980) 121.
[32] J.-P.L.A Gatellier, J.W. de Leeuw, J.S. Sinninghe Damsté, S. Derenne, C. Largeau and P. Metzger, Geochim. Cosmochim. Acta, 57 (1993) 2053.
[33] K.A. Gould, Fuel, 57 (1978) 756.
[34] J.L. Faulon, M. Vandenbroucke, J.M. Drappier, F. Behar and M. Romero, Org. Geochem. 16 (1989) 981.
[35] J.S. Sinninghe Damsté, F.X.C de las Heras and J.W. de Leeuw, J. Chromatogr., 607 (1992) 361.
[36] P. Metzger, C. Largeau and E. Casadevall, in W. Herz et al. (Eds.), Progress in the Chemistry of Organic Natural Products, Springer Verlag, New York, 1991, p. 1.
[37] J.S. Sinninghe Damsté, A.C. Kock-van Dalen, J.W. de Leeuw and P.A. Schenck, J. Chromatogr., 435 (1988) 435.
[38] J. Espitalié, M. Madec and B. Tissot, Am. Geol. Bull., 64 (1980) 59.
[39] A.C. Buchanan III, P.F. Britt and C.A. Biggs, Energy Fuels, 6 (1992) 110.